Gastrointestinal microbiota and local inflammation during oxazolone-induced dermatitis in BALB/cA Mice

Lundberg, Randi; Knoth Clausen, Susanne ; Pang, Wanyong; Nielsen, Dennis Sandris; Möller, Kristian; Josefsen, Knud Elnegaard; Hansen, Axel Jacob Kornerup

Original Research

Gastrointestinal Microbiota and Local Inflammation during Oxazolone-induced Dermatitis in BALB/cA Mice

Randi Lundberg,[1,*] Susanne K Clausen,[3] Wanyong Pang,[1] Dennis S Nielsen,[2] Kristian Möller,[3] Knud E Josefsen,[4] and Axel K Hansen[1]

At present, laboratory animals are not standardized with regard to the gastrointestinal microbiota (GM), but differences in this feature may alter various parameters in animal models. We hypothesized that variation in the GM correlated with variation in clinical parameters of a murine oxazolone-induced skin inflammation model of atopic dermatitis. BALB/cA mice were sensitized with oxazolone over a 28-d period and variation in gastrointestinal microbiota in fecal and cecal samples was assessed by PCR-denaturing gradient gel electrophoresis. Clinical parameters included transepidermal water loss, ear thickness, inflammatory factors in ear tissue and plasma, and histopathologic evaluation. The fecal microbiota before induction of skin inflammation strongly correlated with the levels of some proinflammatory cytokines (IFNγ, IL1β, IL12, and TNFα), the antiinflammatory cytokines IL4 and IL10, and the chemokine KC/GRO that were measured in ear samples at study termination. Cecal microbiota at termination correlated with ear thickness and transepidermal water loss. There was no correlation between cytokine responses and ear thickness or transepidermal water loss. In addition, GM changed during the study period in the oxazolone-treated mice, whereas this was not the case for the control mice. The current study shows that the GM of mice influences the development of oxazolone-induced skin inflammation and that the model itself likely induces a pathophysiologic response that alters the composition of the GM.

Abbreviations: AD, atopic dermatitis; CRP, C-reactive protein; GM, gastrointestinal microbiota; KC/GRO, keratinocyte-derived chemokine/growth-related oncogene; PCA, principal component analysis; TEWL, transepidermal water loss.

Interest in how the gastrointestinal microbiota (GM) stimulates the immune system and thereby contributes to the development of immunologic and inflammatory diseases has increased during recent years. In several animal models, including those for type 1 diabetes,[20,21,29] type 2 diabetes,[4,52] and colitis,[45] disease expression is influenced strongly by the GM.[6,32] The effect of the GM on animal models has been demonstrated by using antibiotic-treated[6] or germ-free mice, which can express increased or decreased disease incidence depending on the model.[32] Germ-free conditions are rather dramatic compared with the smaller deviations between the GM of individuals observed in mice purchased from commercial breeders,[26] as not only the complete absence of microbes, but also the balance between different species affect the immune system, for example, gram-positive bacteria from human GM induce considerably higher levels of the Th1 cytokines IL12 and TNFα in human neonatal cells than do gram-negative bacteria;[32] Th17 cells accumulate only in the presence of some members of segmented filamentous bacteria;[27] and regulatory T cells may in-

crease in number because of the presence of specific species of lactobacilli and *Bifidobacteria*.[13,34] In addition, the composition of the GM strongly affects disease development in humans.[46]

Variations in the GM can be investigated using by a molecular fingerprinting method, denaturing gradient gel electrophoresis, and a mathematical model, principal component analysis (PCA). In denaturing gradient gel electrophoresis, PCR products of similar size are separated on a gel with a denaturing gradient, resulting in a pattern of bands in which each band ideally represents a bacterial population.[17] To perform PCA on the band patterns, the areas of the highest discrimination are calculated—that is, each sample is scored quantitatively on a scale that expresses how different the samples are. The components with the highest, second-highest, and third-highest discrimination can then be put into a 3D plot to illustrate whether they cluster according to groups or just spread randomly in the plot.[49] In theory, the plot can involve an infinite number of axes, but for visual reasons, those 3 with the highest discriminatory capability typically are chosen, because significant differences, if any, most likely will be found on one of these. The PC values on the axes of the PCA plot are arbitrary, but can be used for calculating differences between groups of band patterns (that is, GM profiles) or in a regression analysis to show whether GM composition predicts other parameters.

If variations in GM composition are correlated with disease expression in mice, improved control of the GM may be a potential tool for reducing group sizes in animal studies. The composition of the GM varies substantially between even inbred mice, which may have an interindividual similarity in their GM of less than 80%[26] due to both genetic and environmental reasons.[25,42] It is therefore reasonable to assume that if variation in the GM composition of mouse models can be better controlled, it also will be possible to reduce interindividual variation and thereby group sizes in mouse studies.

Atopic dermatitis (AD) is an inflammatory, chronically relapsing, noncontagious and pruritic eczema[10] characterized by xerosis, pruritus, and cutaneous inflammation, which affects up to 20% of children in some geographic areas.[55] Several animal models are available for human AD. Nc/Nga mice spontaneously develop AD-like skin lesions, but only under conventional housing conditions,[36] thereby indicating a correlation with GM composition. Other models involve topical administration of haptens such as oxazolone,[28] a potent contact allergen; a single topical application of oxazolone provokes T cell–mediated delayed type hypersensitivity. During the sensitization phase, the antigen is phagocytized and processed by Langerhans cells and other dedicated antigen presenting cells, which in turn migrate to skin-draining lymph nodes, where they present the antigen to naïve CD4+ T cells.[19] IL12 produced by Langerhans cells results in a differentiation toward a Th1 cytokine milieu.[12] During the elicitation phase, the primed Th1 cells patrol the skin and become activated on meeting the antigen and subsequently initiate an inflammatory response.[19] After 9 or 10 challenges with oxazolone on mouse skin, a phenotype evolves with multiple features resembling human AD.[35] During the chronic phase of oxazolone-induced murine skin inflammation, a Th2-associated cytokine profile with high levels of IL10 dominates in contrast to the early Th1-dominating response with high levels of TNFα and IL12.[18,54] This feature makes this murine model somewhat analogous to early stages of human AD, in which Th2 cytokines dominate in the acute phase, whereas Th1 cytokines dominate in the chronic phase.[23,33] Clinically, the oxazolone model is characterized by monitoring the thickness of the edema-swollen pinnae (ear thickness) and transepidermal water loss (TEWL), which is a well-established measure of skin barrier function in human AD patients.[1,16]

The GM of children with AD is different and less diverse than that of nonallergic children.[5] Differences in the GM of fecal samples of 1-mo-old infants have been shown to precede manifestations of atopic symptoms later in life;[43] other studies have also linked GM to the development of atopic diseases.[24,30,53] We, hypothesized that the composition of the GM influences the development of AD in the oxazolone mouse model.

Materials and Methods

Mice. Housing, maintenance, and experimental procedures were conducted in accordance with the European Convention for the Protection of Vertebrate Animals used for Experimental and Other Scientific Purposes (ETS 123 of 1986)[9] and The Danish Animal Experimentation Act (LBK no. 1306 of 23/11/2007).[37] The study was approved by the Animal Experiments Inspectorate, Ministry of Food, Agriculture and Fisheries, Denmark.

Female BALB/cABomTac mice ($n = 30$; age, 7 wk; Taconic, Ejby, Denmark), screened for infectious agents according to the Murine Pathogen-Free health standard of the breeder and FELASA guidelines,[38] arrived at the facility (LEO Pharma, Ballerup, Denmark) and were allowed to acclimate for 9 d. BALB/cA mice were chosen for the strain's ability to produce robust cellular and humoral immune responses.

Mice were housed in an experimental facility with restricted access, quarantine rules, and control of incoming objects in Eurostandard type III transparent cages (Techniplast, Varese, Italy) with aspen bedding (Tapvei, Kortteinen, Finland) in an individually ventilated Scantainer (Scanbur A/S, Karlslunde, Denmark) with a minimum of 20 air exchanges hourly. Mice received commercial diet (no. 1324, Altromin, Lage, Germany) and bottled tap water without further treatment or additives ad libitum. Cages were enriched with Fun Tunnels (size, mini; Lillico Biotechnology, Hookwood, UK), Des Res. Mouse House (Lillico Biotechnology), nesting material (Sizzle-nest, NOVA-SCB, Sollentuna, Sweden) and aspen bricks (size, M; Tapvei). Bedding, feed, and enrichment materials were not sterilized. Temperature was 20 to 23 °C, relative humidity was 30% to 60%, and lights were on from 0600 to 1800. Three groups of 10 mice each were used: an oxazolone group, a vehicle-only control group, and a baseline group. Animal welfare during the study period was monitored by systematic observations of body weight, piloerection, and general condition.

Induction of skin inflammation. Mice in the oxazolone group were sensitized once on day −7 by topical application of 20 µL 0.8% oxazolone (4-ethoxymethylene-2-phenyl-2-oxazolin-5-one; Sigma-Aldrich, St Louis, MO) dissolved in acetone (Emsure, Merck Chemicals, Darmstadt, Germany) with a pipette on both sides of the right ear while they were restrained by scruffing of the neck. After a week, challenges comprising 20 µL 0.4% oxazolone were performed on days 0, 3, 7, 10, 12, 14, 16, 18, and 20, each time by using a freshly prepared solution (Figure 1). Concurrently, on days 10 through 21, mice in the oxazolone and vehicle-only groups were sham-treated once daily with 20 µL acetone to mimic the model when it is used for efficacy testing; in the way, we ensured that test results could be compared with previous inhouse studies. Mice in the vehicle-only group were sham-sensitized, sham-challenged, and sham-treated with 20 µL acetone topically on both sides of the left and right ear, according to the same time scheme as that for the oxazolone group. The baseline group was not sensitized, challenged, or treated. The dosage regimen was determined based on inhouse experience and previous work with the oxazolone-induced dermatitis model.[35,48]

TEWL and ear thickness. TEWL was measured by using a VapoMeter (Delfin Technologies, Kuopio, Finland) on the right ear on days −7, 10, and 20 before dosing. Room temperature and relative humidity were recorded on each day of TEWL measurements, because these environmental factors influence the VapoMeter's performance.[11] Because temperature and humidity remained within the normal ranges for the facility, VapoMeter measurements were considered valid. Ear thickness was recorded before dosing on the right ear on days 10, 12, 14, 17, 18, and 21 by using an Absolute Digimatic Micrometer (model 547–313, Mitutoyo, Kawasaki, Japan); the same person performed all measurements to ensure consistent pressure and placement of the micrometer.

Plasma cytokines and CRP. Blood was collected terminally by cardiocentesis of mice under isoflurane anesthesia (Baxter, Søllerød, Denmark) on day 0 (baseline group) and day 21 (oxazolone and vehicle-only groups), stabilized in 1.5 mL EDTA anticoagulant-coated test tubes (Eppendorf, Eppendorf, Germany), kept on wet ice, and centrifuged for 10 min at $1000 \times g$ and 4 °C.
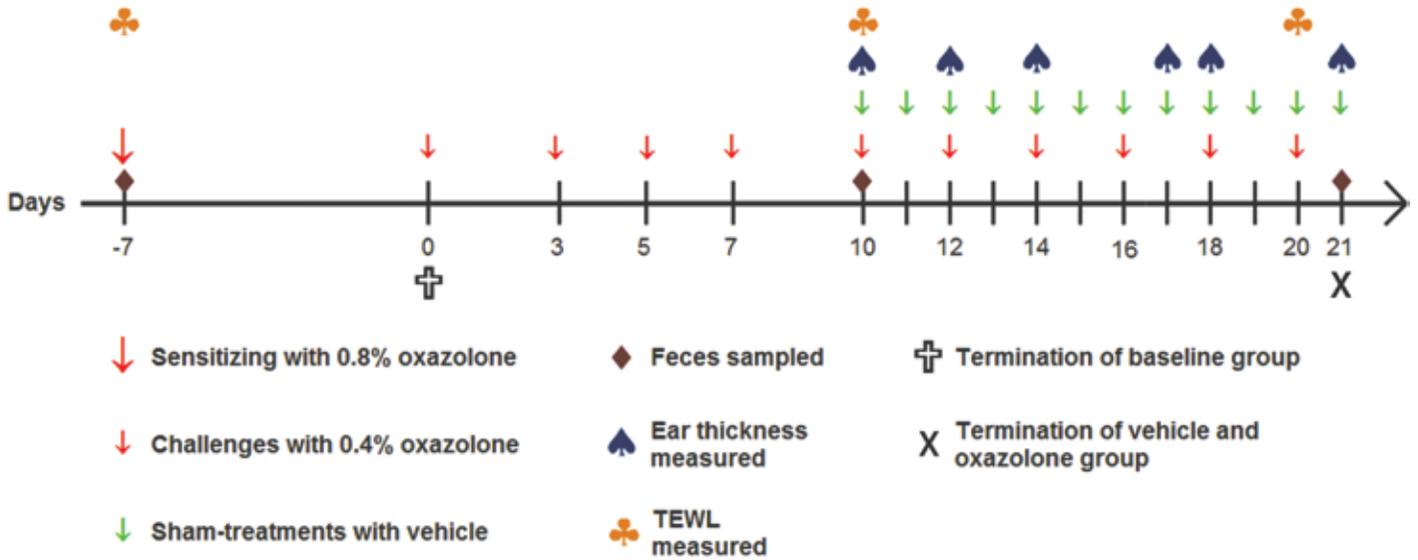
Figure 1. Study timeline. The oxazolone group was sensitized (0.8% oxazolone) on day −7 and challenged (0.4% oxazolone) on days 0, 3, 5, 7, 10, 12, 14, 16, 18, and 20. The vehicle-only group was sham-sensitized with acetone on day −7 and sham-challenged on days 0, 3, 5, 7, 10, 12, 14, 16, 18, and 20. Both groups were sham-treated with acetone on days 10 through 21. Transepidermal water loss (TEWL) was measured on days −7, 10, and 20. Ear thickness was measured on days 10, 12, 14, 17, 18, and 21. Feces were sampled on days −7, 10, and 21. Terminal samples (plasma, cecum, and ear tissue) were harvested on day 0 (baseline group) and day 21 (oxazolone and vehicle groups).

Plasma (70 µL) was isolated and stored at −80 °C. Three blood samples from the oxazolone group were lost due to technical issues. Levels of granulocyte–macrophage colony-stimulating factor, IFNγ, IL1α, IL1β, IL2, IL4, IL5, IL6, IL10, IL12(p70), IL17, and TNFα in plasma were measured by using the Mouse Th1/Th2 10plex FlowCytomix Multiplex kit (Bender Medsystems, Vienna, Austria) and the Mouse IL1β and IL12(p70) Simplex kits (Bender Medsystems). The assay was performed according to the manufacturer's instructions except that we scaled down the volumes of plasma and reagents by 50% due to limited amounts of plasma. The analysis was run on a FACSCanto flow cytometer (BD Biosciences, Brøndby, Denmark), and data were processed by using FlowCytomix Pro 2.3 software (Bender Medsystems). CRP in plasma was evaluated by using the CRP (Mouse) ELISA kit (DRG Diagnostics, Marburg, Germany) according to the manufacturer's instructions; results were read on a Sunrise microplate absorbance reader (Tecan, Männedorf, Switzerland).

Ear tissue cytokines and histology. The noninflamed left and right pinnae of mice in the vehicle-only group and the inflamed right pinnae of mice in the oxazolone group were sampled on day 21 by using an 8-mm disposable dermal biopsy punch (Miltex GmbH, Ratingen, Germany). A 3-mm punch biopsy (Miltex) for histology was taken from the middle of the 8-mm biopsy and preserved in formaldehyde (10%). The remaining biopsy tissue was snap-frozen in liquid nitrogen in a cryotube (Nunc, Roskilde, Denmark) and stored at −80 °C. On the day of analysis, the biopsies were kept cold constantly. Lysis buffer consisting of 10.6 mL 1×PBS without calcium and magnesium (Invitrogen, Life Technologies, Carlsbad), 1 Complete EDTA-free Protease Inhibitor Cocktail tablet (Roche Diagnostics, Hvid-ovre, Denmark), 400 µL NP40 detergent, and 100 µL 1mM $Na_3VO_4^+$ (a phosphatase inhibitor) was prepared. Each biopsy was placed in 200 µL lysis buffer in precooled Precellys (Bertin Technologies, Orleans, France) tubes with ceramic beads and homogenized on a Precellys 24 instrument (Bertin Technologies) at 6800 rpm twice for 15 s each,

with a 30-s pause between sessions to avoid heating. A maximal temperature of 4 °C during homogenization was maintained by using a Cryolys cooling apparatus (Bertin Technologies). The homogenized tissue was centrifuged for 15 min at $15,000 \times g$ and the supernatant used for cytokine analysis. Levels of IFNγ, IL1β, IL2, IL4, IL5, keratinocyte-derived chemokine/growth-related oncogene (KC/GRO), IL10, IL12 (total), and TNFα were analyzed by using the Multispot Mouse Th1/Th2 9plex Assay (Meso Scale Discovery, Gaithersburg); results were read on a SECTOR Imager 6000 (Meso Scale Discovery). The plate was blocked for 1 h by using 150 µL Calibrator Buffer (Meso Scale Discovery) with vigorous shaking at room temperature and then washed 3 times with 150 µL PBS containing 0.05% Tween 20 (Roche Diagnostics) per well. Calibrator-treated sample (25 µL) was added to each well, and the plate was incubated at room temperature with shaking for 2 h; 25 µL of 1× Detection Antibody (Meso Scale Discovery) was added to each well, the plate was incubated with shaking for 2 h at room temperature, wells were washed 3 times with 150 µL PBS containing 0.05% Tween 20 per well, and 150 µL 2× Read Buffer (Meso Scale Discovery) was added to each well. The biopsies preserved in formaldehyde were embedded in paraffin, sliced, and stained with hematoxylin and eosin, and the type of inflammation was evaluated.

Fecal and cecal samples. Fecal samples were collected on days −7, 10, and 21 by letting mice defecate spontaneously into an autoclaved 1.5-mL test tube (Eppendorf) during restraint. Cecal samples were collected on day 0 (baseline group) and day 21 (oxazolone and vehicle-only groups) by aseptic excision immediately after euthanasia; samples were put in autoclaved 1.5-mL test tubes (Eppendorf). Fecal and cecal samples were placed immediately on wet ice and stored at −80 °C within 30 min of collection. DNA was extracted by using the QIAamp DNA Stool Mini Kit (Qiagen, Hilden, Germany) according to the manufacturer's protocol for isolation of DNA for pathogen detection. Before extraction, cecal tissue samples were homogenized by using a FastPrep
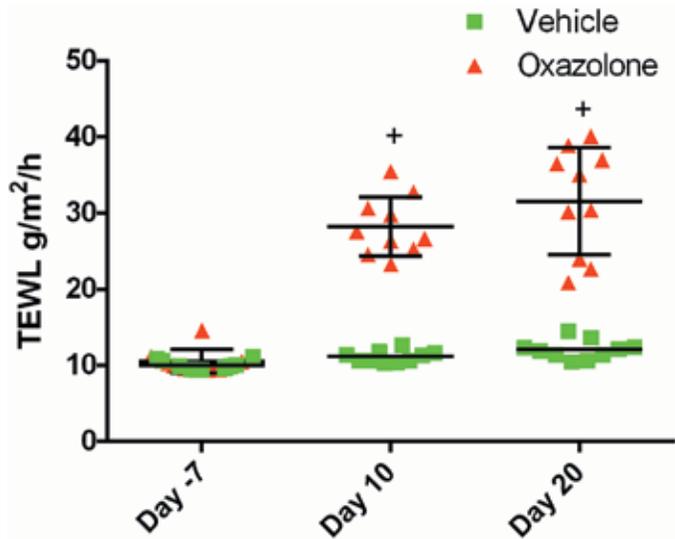
Figure 2. Transepidermal water loss (TEWL; g/m²/h) in the right ear (mean, SD) of mice dosed with vehicle or oxazolone showing significantly (+, $P < 0.0001$) higher TEWL in the oxazolone group on days 10 and 20.
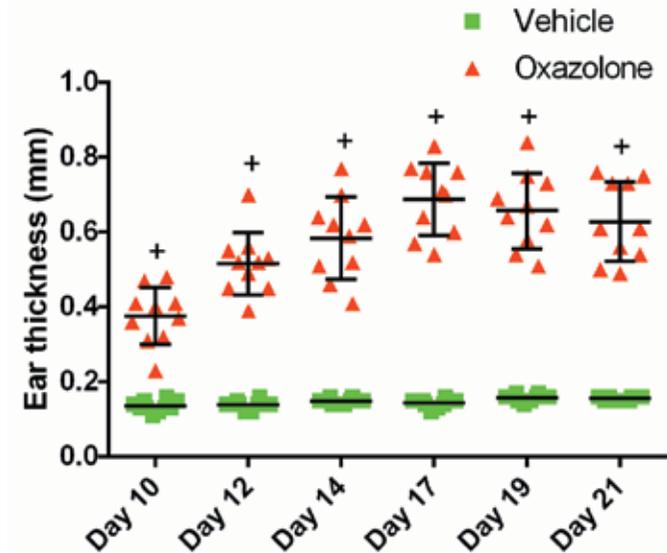

Figure 3. Ear thickness (mm) on the right ear (mean, SD) of mice dosed with vehicle or oxazolone. Compared with that in the vehicle-only group, ear thickness is greater (+, $P < 0.0001$) in the oxazolone group at all time points (days 10, 12, 14, 17, 19, and 21).

FP120 Cell Disrupter (QBiogene, MP Biomedicals, Ilkirch, France) for 45 s at 6 m/s. Quality and concentration of the extracted DNA was checked on a NanoDrop 1000 Spectrophotometer (Thermo Scientific). DNA extracts from fecal and cecal samples were stored at −40 °C.

Gut microbiota characterization. The V3 region of the bacterial 16S rRNA gene was amplified by PCR using the universal primers PRBA338f (Eurofins MWG Operon, Ebersberg, Germany) and PRUN518r[41] (Eurofins MWG Operon). All reactions were done in a 50-µL volume containing 5 µL 10× HotMasterTaq Buffer (5 Prime, Hamburg, Germany), 12 µL dNTPs (1.25 mM, Bioline, Risskov, Denmark), 0.25 µL 1.25 U HotMasterTaq DNA Poly-

merase (5 Prime), 10 pmol of each primer, 1 µL bovine serum albumin (5 µl/mL; Sigma-Aldrich), approximately 50 ng DNA, and sufficient ultrapure water to bring the reaction volume to 50 µL. PCR amplification was performed on a GeneAmp PCR System 9700 (Applied Biosystems, Life Technologies, Carlsbad, CA) with initial denaturation at 95 °C for 5 min followed by 30 cycles of denaturation at 95 °C for 30 s, annealing at 60 °C for 30 s, and extension at 72 °C for 40 s and a final elongation step at 72 °C for 10 min. The PCR product (approximately 230 bp) was checked by electrophoresis on a 2% agarose gel at 100 to 120 V for 20 min. The gel was stained with ethidium bromide (4 µg/mL) for 10 min and visualized on an AlphaImager HP (Cell Biosciences, Santa Clara). PCR products were separated by denaturing gradient gel electrophoresis using the PhorU-2 system (INGENY, Amundsenweg, Netherlands) according to the manufacturer's instructions. The acrylamide concentration in the gel was 9%, and the linear denaturation gradient was 30% to 65%. For each well, 20 µL of the PCR product was mixed with 3.75 µL 6× DNA loading dye (Fermentas, Thermo Fisher Scientific, GlenBurnie, MD) and loaded on the gel. In addition, a standard consisting of mixed PCR products representing mouse fecal samples with diverse bands was loaded to enable accurate alignment of lanes and bands within and between gels. Electrophoresis was performed in 0.5×TAE buffer at 60 °C for 16 h at 120 V. The gels were stained by using a 1:10,000 SYBR Gold solution (Invitrogen, Life Technologies) in 0.5×TAE for 1 h and photographed under UV transillumination (EDAS, Eastman Kodak, Rochester, NY).

Statistical analysis. Denaturing gradient gel electrophoresis profiles were analyzed by using BioNumerics version 4.5 (Applied Maths, Sint-Martens-Latem, Belgium) to calculate the Dice coefficient of similarity (with a band position tolerance and optimization of 1%) and to apply the unweighted pair-group method with an arithmetic averages clustering algorithm for dendrogram construction. 3D principal component analysis (PCA) plots were made by band-matching of data from denaturing gradient gel electrophoresis, and values of PC1, PC2, and PC3 were obtained from plots and correlated with clinical parameters (TEWL, ear thickness, ear tissue cytokines, plasma cytokines, and CRP). Within the oxazolone group, regressions were made between the combined PC1–PC2–PC3 and each clinical data set. Regressions were checked for validity by removal of a random sample of data followed by regression analysis of the remaining data. Regressions also were performed for correlations between cytokine data and TEWL as well as ear thickness. Clinical parameters and PC values were compared between groups by ANOVA in GraphPad Prism version 5.04 for Windows (GraphPad Software, La Jolla, CA). All data were tested for normality by the D'Agostino and Pearson omnibus normality test. For normally distributed data, a Student *t* test or one-way ANOVA was used, followed by the Bonferroni multiple comparison test. For data that did not meet normality criteria, the Mann–Whitney *U* test or Kruskal–Wallis one-way ANOVA was used, followed by the Dunn multiple comparison test. Regressions were performed by using Statistical Software version 16.1.1 (Minitab, State College, PA). The confidence level was 95% for all tests. All parametric values are reported as mean ± 1 SD.

Results

The oxazolone group showed overt signs of inflammation, namely redness and swelling, along with an increase in TEWL
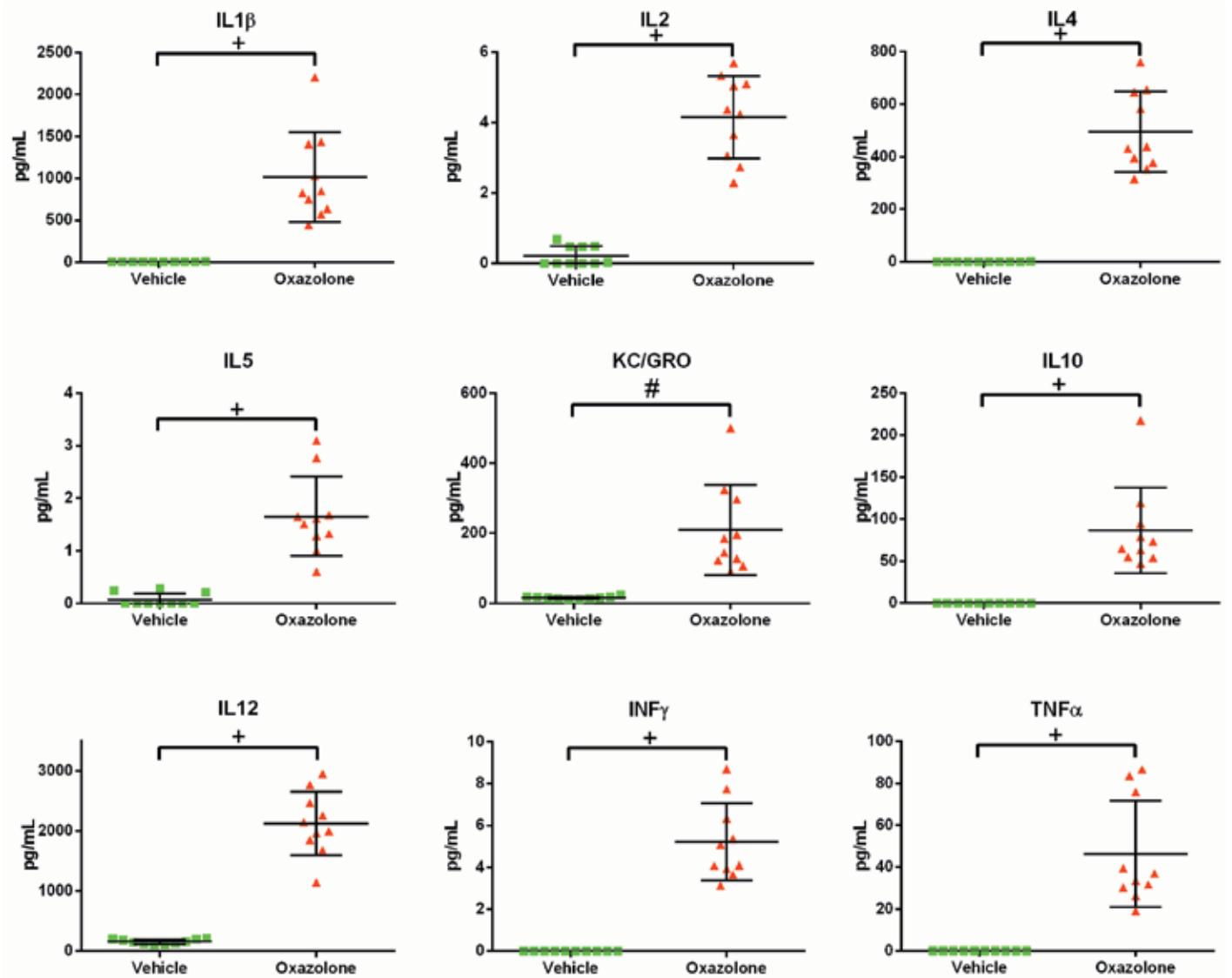
Figure 4. Cytokine levels (mean ± 1 SD) in ear tissue on day 21 in mice dosed with vehicle or oxazolone. All cytokines are higher (#, $P < 0.001$ for KC/GRO; +, $P < 0.0001$ for IL1β, IL2, IL4, IL5, IL10, IL12, INFγ, and TNFα) in the oxazolone group.

on days 10 and 20 ($P < 0.0001$ for both days; Figure 2). On day 21, after 10 oxazolone challenges, epidermal ear thickness (mean ± 1 SD) in the oxazolone group was 0.63 ± 0.11 mm compared with 0.16 ± 0.01 mm in the vehicle-only group ($P < 0.0001$; Figure 3), and all ear tissue cytokines were higher in the oxazolone group ($P < 0.001$ for KC/GRO; $P < 0.0001$ for IL1β, IL2, IL4, IL5, IL10, IL12, INFγ, and TNFα; Figure 4). Histologically, oxazolone-treated ears were characterized by severe, chronic–active, diffuse, suppurative dermatitis in both the epidermal and dermal layers. A mixed infiltration of mainly granulocytes with moderate numbers of lymphocytes, mast cells, macrophages, and eosinophils was present. Hyperkeratosis and parakeratosis in the stratum corneum, hypergranulosis in the stratum granulosum and hyperplasia of the stratum spinosum (acanthosis), and intercellular epidermal edema (spongiosis) were prominent (Figure 5). No deviations from normal were noted regarding body weight, piloerection, and general behavior. Scratching behavior was not seen, either

indirectly in the form of wounds or directly during cageside observations.

Plasma levels of IL6 were higher ($P < 0.01$) in the baseline group compared with the oxazolone group (Figure 6). CRP was higher ($P < 0.01$) in the oxazolone group (44.88 ng/mL) compared with the baseline (38.68 ng/mL) and vehicle-only (38.60 ng/mL) groups (Figure 7). No differences were detected between groups with regard to plasma levels of granulocyte–macrophage colony-stimulating factor, IFNγ, IL1α, IL1β, IL2, IL4, IL5, IL10, IL12(p70), IL17, and TNFα (Figure 6). There was significant correlation between the combined PC1–PC2–PC3 of the fecal samples from day −7 and the final levels of the ear tissue cytokines IFNγ ($P < 0.001$, $r^2 = 0.93$), IL1β ($P < 0.01$, $r^2 = 0.83$), IL4 ($P < 0.05$, $r^2 = 0.74$), IL8 ($P < 0.01$, $r^2 = 0.88$), IL10 ($P < 0.01$, $r^2 = 0.86$), IL12 ($P < 0.05$, $r^2 = 0.71$), and TNFα ($P < 0.01$, $r^2 = 0.87$; Table 1). However, the correlation with IL4 disappeared by removing a random data set. There was also significant correlation between the combined PC1–PC2–PC3 of the cecal microbiota and TEWL ($P < 0.05$, $r^2 = 0.76$) as well as
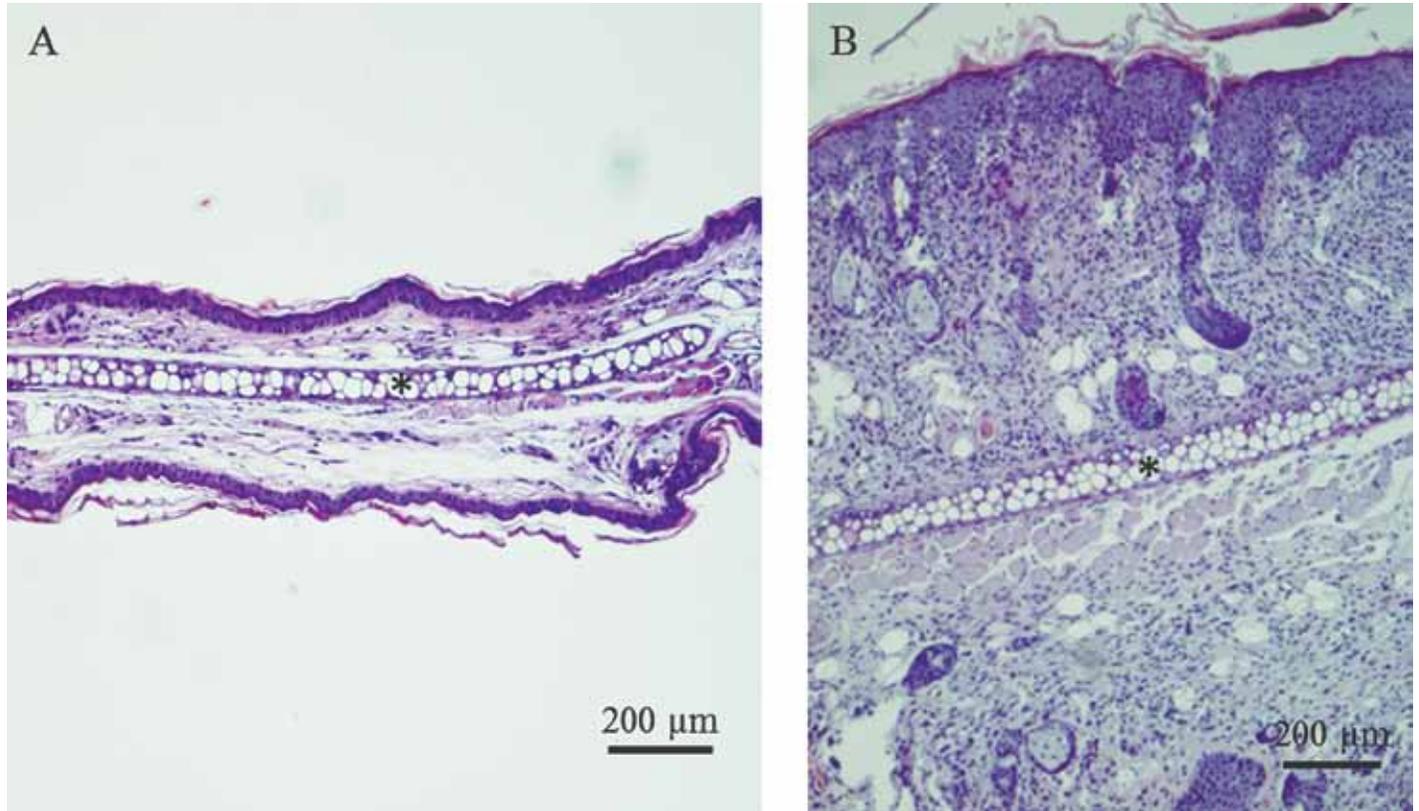
Figure 5. Cross-sections of pinnae from 1 mouse each from (A) the vehicle-only group and (B) the oxazolone group. (A) Normal epidermis, dermis, and subcutis. (B) Hyperkeratosis and parakeratosis in stratum corneum, hypergranulosis in stratum granulosum, and hyperplasia of stratum spinosum (acanthosis); intercellular epidermal edema (spongiosis), and mixed infiltration in both epidermis and dermis consisting mainly of neutrophil granulocytes. *, Auricular cartilage. Hematoxylin and eosin stain; magnification, 10×.

ear thickness ($P < 0.05$, $r^2 = 0.80$) and between ear thickness and TEWL ($P < 0.05$, $r^2 = 0.44$), but none of the cytokines in either plasma or ear tissue correlated with ear thickness or TEWL.

The cecal GM was clearly separated into 2 groups by PC1 consisting of the oxazolone group compared with the vehicle-only and baseline groups taken together ($P < 0.01$; Figure 8), whereas the vehicle-only group did not cluster significantly different from the baseline group. The fecal GM in the oxazolone group changed during the study period, leading to significantly ($P < 0.0001$) different clustering of samples by PC1 between days –7 and 21; this change in GM was not observed in the vehicle group (Figure 9).

Discussion

Topical administration of oxazolone induced immense local inflammation in the pinnae of our mice. TEWL and ear thickness increased in the oxazolone-treated mice, which also showed clear responses in all ear tissue cytokine levels compared with those of the vehicle-only group. The cytokine picture was a mixture of proinflammatory responses, including those in IL1, IL6, IL12, TNFα, and IFNγ, and antiinflammatory responses, such as those involving IL4 and IL10. These results suggest that this model of atopic dermatitis is in transition from an acute to chronic disease phase.

The initial composition of the fecal microbiota and the cytokine response in the ear tissue of oxazolone-treated mice related in that levels of the proinflammatory cytokines IFNγ, IL1β, IL12,

and TNFα; the antiinflammatory cytokines IL4 and IL10; and the chemokine KC/GRO paralleled the degree of variation in the GM before skin inflammation was induced. Several studies have demonstrated that the GM is a factor in the development of AD in humans,[43] but to our knowledge this study shows for the first time that GM composition can be used to predict parameter expression in an animal model of AD. Our findings, therefore, add to the increasing awareness that variation in GM accounts for much of the variation observed in such inflammatory models.[6] Other models, including several transgenic and knockout mouse strains, develop various types of spontaneous dermatitis,[28] and it may be fruitful to investigate the correlation between AD and GM in these systems. Another option might be to inoculate mice with a specific GM that has particular relevance for the model.[22]

In the current study, GM composition seemed to have the greatest effect on the cytokine levels in samples of ear tissue, whereas other parameters—ear thickness and TEWL—did not correlate with either GM or the inflammatory response in the ear. In this context, it should be remembered that the oxazolone-treated mouse model is chemically induced, and human patients with AD do not develop disease as a response to having a hapten applied repeatedly to the skin. Our study suggests that factors other than inflammation contribute markedly to the macroscopic signs of dermatitis, and these factors very likely reflect the repeated application of a chemical to the skin.

The composition of the fecal GM varied during the experimental period in the oxazolone-treated mice but not in the vehicle-
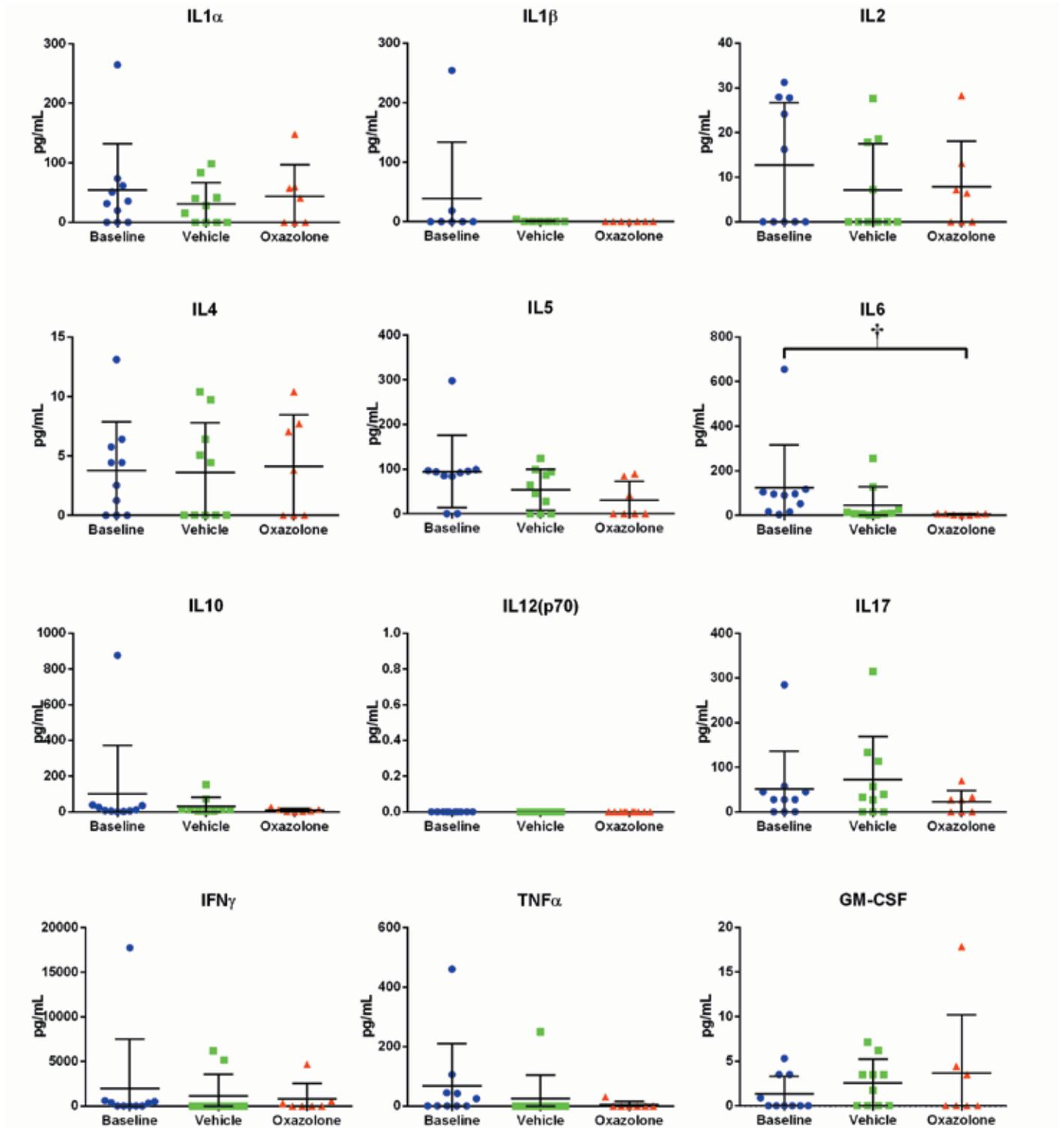
Figure 6. Plasma cytokine levels (mean ± 1 SD) in nondosed (baseline), vehicle- and oxazolone-dosed mice measured on day 21. IL6 is higher (†, $P <$ 0.01) in the baseline group than in the oxazolone group. For IL1α, IL1β, IL2, IL4, IL5, IL10, IL12(p70), IL17, INFγ, TNFα and granulocyte–macrophage colony-stimulating factor (GM-CSF) differences between the groups are nonsignificant.

treated mice. In cecal samples, the GM of oxazolone-treated mice differed from those of the vehicle-treated and baseline mice, which did not differ from each other, even though the baseline and vehicle-only samples were obtained 20 d apart. These data suggest that the ear inflammation may have triggered a stress response in the mice, which subsequently caused perturbations in GM during the study period. Despite the lack of clinical signs of decreased animal welfare, we cannot exclude the possibility that
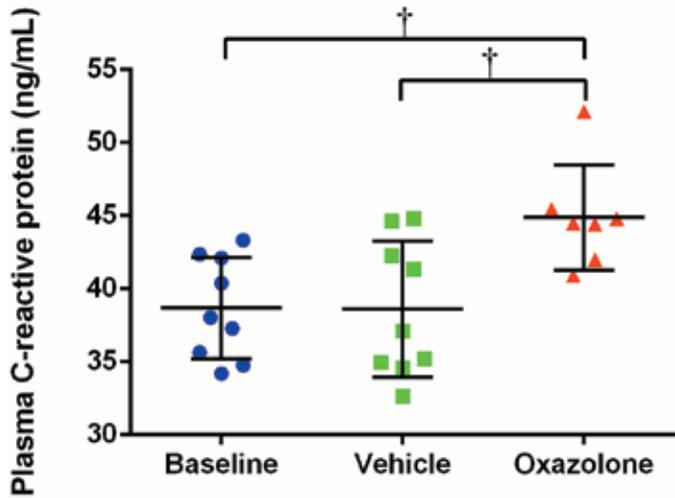
Figure 7. Plasma levels of C-reactive protein (mean ± 1 SD) in plasma of nondosed (baseline), vehicle- and oxazolone-dosed mice measured on day 21. Plasma C-reactive protein is higher (†, $P < 0.01$) in the oxazolone group.

Table 1. Correlation of initial fecal gastrointestinal microbiota composition and local cytokine levels in ear tissue from the oxazolone group at study termination

	IFNγ	KC/GRO	TNFα	IL1β	IL2	IL4	IL5	IL10	IL12
r^2	0.93	0.88	0.87	0.83	0.07	0.74	0.47	0.86	0.71
P	0.001	0.01	0.01	0.01	ns	0.05[a]	ns	0.01	0.05

ns, nonsignificant.

Regression analysis was performed on the combined principal components (PC1, PC2, PC3) of feces from day −7 and correlated against cytokine levels in ear tissue on day 21.

[a]The significance of the correlation between fecal composition and local ear IL4 is questionable, because this significance disappears after removal of a random data set; this effect did not occur with any other cytokine.

the immense inflammation and pronounced edema in the pinnae caused some level of pain and irritation. The GM is believed to influence pain perception[47] and seems to be necessary for mice to develop inflammatory hypernociception.[2] Restraint-associated stress causes exaggerated increases in ACTH and corticosterone levels in germ-free but not SPF mice, and this effect can be reversed by monoassociation with a single organism, *Bifidobacterium infantis*,[50] a predominant bacterium in the infant gut and a commonly used probiotic organism.[40] In addition, it recently was demonstrated that mice exposed to a social-disruption stressor displayed changes in the composition, diversity, and quantity of the GM.[3] Hapten-induced ear inflammation in nonobese diabetic mice reduces the incidence of type 1 diabetes,[14,15] the incidence of which also is known to be associated with the GM.[7,20,21] The mechanism behind this association may be that the dermatitis stresses the mice, leading to a change in the GM composition and thereby a difference in the incidence of diabetes. Alternatively, in the present study, oxazolone itself may have disturbed the bacterial composition in the gastrointestinal tract, for example, via the oral route due to cagemates licking each other's ears.

IL6 was higher in the untreated baseline group compared with the oxazolone and vehicle-only groups. This difference may be
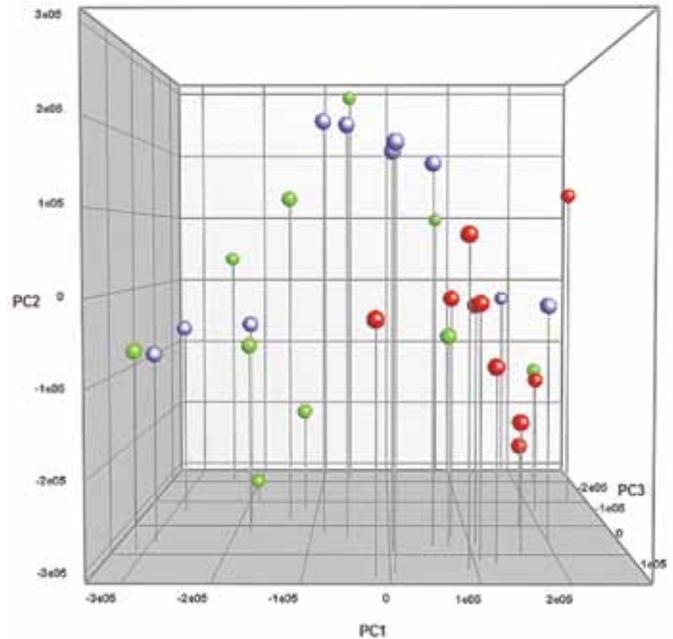

Figure 8. Principal component (PC) analysis plot of cecal gastrointestinal microbiota from nondosed baseline mice (blue bullets), vehicle-dosed mice (green bullets), and oxazolone-dosed mice (red bullets). Clusters representing the oxazolone-treated group differed significantly ($P < 0.05$) from those corresponding to the combined vehicle-only and baseline groups on PC1.

incidental because TNFα and IL1 were not different, as would be expected given the lack of increases in the IL6 levels of the oxazolone- and vehicle-treated mice. However, because IL6 can be secreted by macrophages in response to microbe-associated molecular patterns, it represents one of the key pathways through which the GM could act on the immune system,[51] and increases in IL6 frequently are associated with stress.[39] Increased IL6 levels might have been induced through a very acute reaction in the baseline group that was caused by stress associated with terminal sampling. The chronic, local inflammation may also have had affected systemic levels of CRP, which were increased in oxazolone-treated mice. Murine CRP is not a major acute-phase protein but is rather a trace protein that is detectable only at very low levels even during acute inflammation.[44,56] CRP, however, is involved in complement binding, macrophage activation, and innate immunity, and thus a link to the GM composition still may exist.[44] Although levels of CRP around 45 ng/mL are low,[8] chronic unpredictable stress increases CRP in ApoE knockout mice to levels within the same range, but because CRP also increases IL6 levels,[57] these 2 parameters are somewhat contradictory.

In conclusion, our study shows that the GM of mice is related to the development of oxazolone-induced skin inflammation. In addition, generation of the inflammation likely induces a pathophysiologic response that alters the GM composition.
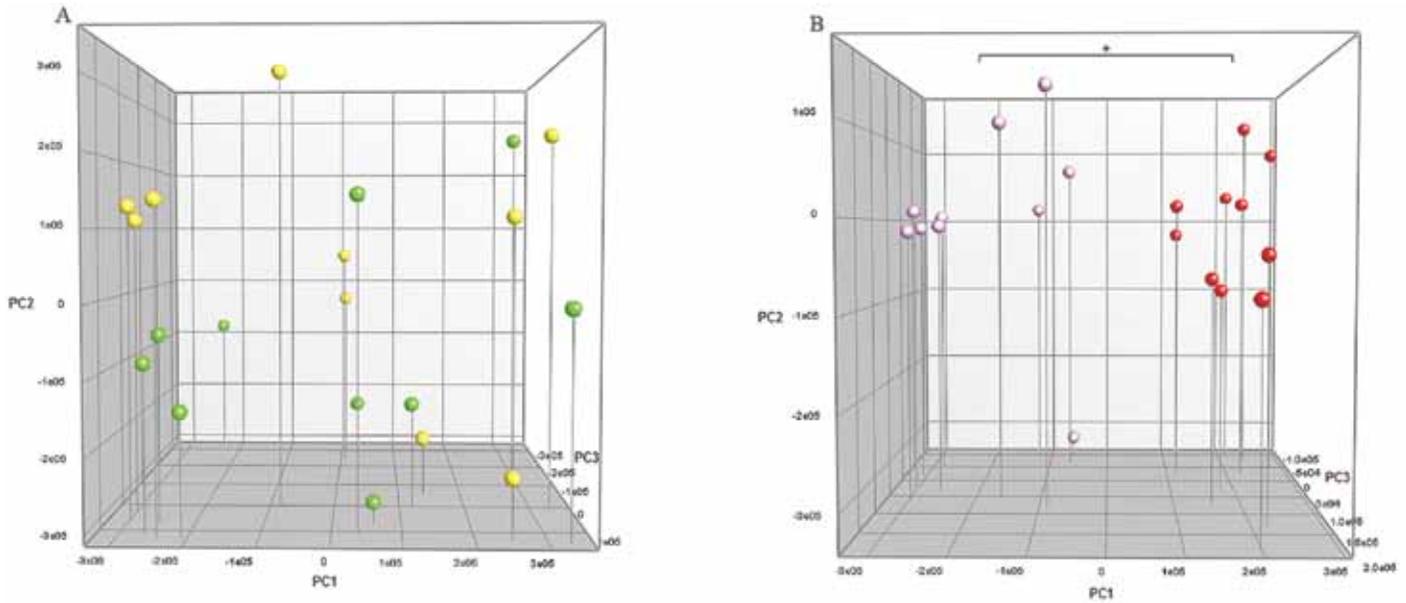
Figure 9. Principal component (PC) analysis plots of fecal gastrointestinal microbiota at baseline and at termination of the study. (A) Vehicle-dosed mice (green bullets, day −7; yellow bullets, day 21). (B) Oxazolone-dosed mice (red bullets, day −7; pink bullets, day 21). The oxazolone-dosed mice showed significant (+, $P < 0.0001$) clustering on PC1 due to a difference between the day −7 and day 21 samples.

References

1. **Addor FAS, Aoki V.** 2010. Skin barrier in atopic dermatitis. An Bras Dermatol **85:**184–194.

2. **Amaral FA, Sachs D, Costa VV, Fagundes CT, Cisalpino D, Cunha TM, Ferreira SH, Cunha FQ, Silva TA, Nicoli JR, Vieira LQ, Souza DG, Teixeira MM.** 2008. Commensal microbiota is fundamental for the development of inflammatory pain. Proc Natl Acad Sci USA **105:**2193–2197.

3. **Bailey MT, Dowd SE, Galley JD, Hufnagle AR, Allen RG, Lyte M.** 2011. Exposure to a social stressor alters the structure of the intestinal microbiota: implications for stressor-induced immunomodulation. Brain Behav Immun **25:**397–407.

4. **Bech-Nielsen GV, Hansen CH, Hufeldt MR, Nielsen DS, Aasted B, Vogensen FK, Midtvedt T, Hansen AK.** 2012. Manipulation of the gut microbiota in C57BL/6 mice changes glucose tolerance without affecting weight development and gut mucosal immunity. Res Vet Sci **92:**501–508.

5. **Bjorksten B, Sepp E, Julge K, Voor T, Mikelsaar M.** 2001. Allergy development and the intestinal microflora during the first year of life. J Allergy Clin Immunol **108:**516–520.

6. **Bleich A, Hansen AK.** 2012. Time to include the gut microbiota in the hygienic standardisation of laboratory rodents. Comp Immunol Microbiol Infect Dis **35:**81–92.

7. **Buschard K, Pedersen C, Hansen SV, Hageman I, Aaen K, Bendtzen K.** 1992. Anti-diabetogenic effect of fusidic acid in diabetes prone Bb rats. Autoimmunity **14:**101–104.

8. **Clyne B, Olshaker JS.** 1999. The C-reactive protein. J Emerg Med **17:**1019–1025.

9. **Council of the European Communities.** Council Directive 86/609/EEC of 24 November 1986 on the approximation of laws, regulations and administrative provisions of the Member States regarding the protection of animals used for experimental and other scientific purposes. Off J Eur Communities **L358:**1–28.

10. **De Benedetto A, Agnihothri R, McGirt LY, Bankova LG, Beck LA.** 2009. Atopic dermatitis: a disease caused by innate immune defects? J Invest Dermatol **129:**14–30.

11. **De Paepe K, Houben E, Adam R, Wiesemann F, Rogiers V.** 2005. Validation of the VapoMeter, a closed unventilated chamber system to assess transepidermal water loss vs. the open chamber Tewameter. Skin Res Technol **11:**61–69.

12. **Eisenbarth SC, Piggott DA, Bottomly K.** 2003. The master regulators of allergic inflammation: dendritic cells in Th2 sensitization. Curr Opin Immunol **15:**620–626.

13. **Ejsing-Duun M, Josephsen J, Aasted B, Buschard K, Hansen AK.** 2008. Dietary gluten reduces the number of intestinal regulatory T cells in mice. Scand J Immunol **67:**553–559.

14. **Engkilde K, Buschard K, Hansen AK, Menne T, Johansen JD.** 2010. Prevention of diabetes in NOD mice by repeated exposures to a contact allergen inducing a subclinical dermatitis. PLoS ONE **5:**e10591.

15. **Engkilde K, Johansen JD, Hansen AK, Menne T, Buschard K.** 2011. Prevention of type 1 diabetes by inducing subclinical dermatitis on a small area. Diabetes Metab Res Rev **27:**954–958.

16. **Fluhr JW, Feingold KR, Elias PM.** 2006. Transepidermal water loss reflects permeability barrier status: validation in human and rodent in vivo and ex vivo models. Exp Dermatol **15:**483–492.

17. **Fromin N, Hamelin J, Tarnawski S, Roesti D, Jourdain-Miserez K, Forestier N, Teyssier-Cuvelle S, Gillet F, Aragno M, Rossi P.** 2002. Statistical analysis of denaturing gel electrophoresis (DGE) fingerprinting patterns. Environ Microbiol **4:**634–643.

18. **Fujii Y, Takeuchi H, Sakuma S, Sengoku T, Takakura S.** 2009. Characterization of a 2,4-dinitrochlorobenzene-induced chronic dermatitis model in rats. Skin Pharmacol Physiol **22:**240–247.

19. **Grabbe S, Schwarz T.** 1998. Immunoregulatory mechanisms involved in elicitation of allergic contact hypersensitivity. Immunol Today **19:**37–44.

20. **Hansen AK, Ling F, Kaas A, Funda DP, Farlov H, Buschard K.** 2006. Diabetes preventive gluten-free diet decreases the number of caecal bacteria in nonobese diabetic mice. Diabetes Metab Res Rev **22:**220–225.

21. **Hansen CHF, Krych L, Nielsen DS, Vogensen FK, Hansen LH, Sørensen SJ, Hansen AK.** 2012. Early life treatment with vancomycin propagates *Akkermansia muciniphila* and reduces diabetes incidence in nonobese diabetic (NOD) mice. Diabetologia. Epub ahead of print.

22. **Hansen CHF, Nielsen DS, Kverka M, Zakostelska Z, Klimesova K, Hudcovic T, Tlaskalova-Hogenova H, Hansen AK.** 2012. Patterns

of early gut colonization shape future immune responses of the host. PLoS ONE **7:**e34043.

23. **Homey B, Steinhoff M, Ruzicka T, Leung DYM.** 2006. Cytokines and chemokines orchestrate atopic skin inflammation. J Allergy Clin Immunol **118:**178–189.

24. **Hong PY, Lee BW, Aw M, Shek LPC, Yap GC, Chua KY, Liu WT.** 2010. Comparative analysis of fecal microbiota in infants with and without eczema. PLoS ONE **5:**e9964 .

25. **Hufeldt MR, Nielsen DS, Vogensen FK, Midtvedt T, Hansen AK.** 2010. Family relationship of female breeders reduce the systematic interindividual variation in the gut microbiota of inbred laboratory mice. Lab Anim **44:**283–289.

26. **Hufeldt MR, Nielsen DS, Vogensen FK, Midtvedt T, Hansen AK.** 2010. Variation in the gut microbiota of laboratory mice is related to both genetic and environmental factors. Comp Med **60:**336–347.

27. **Ivanov II, Atarashi K, Manel N, Brodie EL, Shima T, Karaoz U, Wei D, Goldfarb KC, Santee CA, Lynch SV, Tanoue T, Imaoka A, Itoh K, Takeda K, Umesaki Y, Honda K, Littman DR.** 2009. Induction of intestinal Th17 cells by segmented filamentous bacteria. Cell **139:**485–498.

28. **Jin H, He R, Oyoshi M, Geha RS.** 2009. Animal models of atopic dermatitis. J Invest Dermatol **129:**31–40.

29. **Hagerman I, Buschard K.** 2002. Antidiabetogenic effect of fusidic acid in diabetes prone BB rats: a sex-dependent organ accumulation of the drug is seen. Pharmacol Toxicol **91:**123–128.

30. **Kalliomaki M, Kirjavainen P, Eerola E, Kero P, Salminen S, Isolauri E.** 2001. Distinct patterns of neonatal gut microflora in infants in whom atopy was and was not developing. J Allergy Clin Immunol **107:**129–134.

31. **Karlsson H, Hessle C, Rudin A.** 2002. Innate immune responses of human neonatal cells to bacteria from the normal gastrointestinal flora. Infect Immun **70:**6688–6696.

32. **Lauritzen L, Hufeldt MR, Aasted B, Hansen CHF, Midtvedt T, Buschard K, Hansen AK.** 2010. The impact of a germ-free perinatal period on the variation in animal models of human inflammatory diseases. Scand J Lab Anim Sci **37:**43–54.

33. **Leung DYM, Boguniewicz M, Howell MD, Nomura I, Hamid OA.** 2004. New insights into atopic dermatitis. J Clin Invest **113:**651–657.

34. **Livingston M, Loach D, Wilson M, Tannock GW, Baird M.** 2010. Gut commensal *Lactobacillus reuteri* 100–23 stimulates an immunoregulatory response. Immunol Cell Biol **88:**99–102.

35. **Man MQ, Hatano Y, Lee SH, Man M, Chang S, Feingold KR, Leung DYM, Holleran W, Uchida Y, Elias PM.** 2008. Characterization of a hapten-induced, murine model with multiple features of atopic dermatitis: structural, immunologic, and biochemical changes following single versus multiple oxazolone challenges. J Invest Dermatol **128:**79–86.

36. **Matsuda H, Watanabe N, Geba GP, Sperl J, Tsudzuki M, Hiroi J, Matsumoto M, Ushio H, Saito S, Askenase PW, Ra C.** 1997. Development of atopic dermatitis-like skin lesion with IgE hyperproduction in NC/Nga mice. Int Immunol **9:**461–466.

37. **Ministry of Justice, Denmark.** 2007. Animal Experimentation Act. LBK no. 1306 of 23/11/2007

38. **Nicklas W, Baneux P, Boot R, Decelle T, Deeny A, Fumanelli M, Illgen-Wilcke B.** 2002. Recommendations for the health monitoring of rodent and rabbit colonies in breeding and experimental units. Lab Anim **36:**20–42.

39. **Nukina H, Sudo N, Aiba Y, Oyama N, Koga Y, Kubo C.** 2001. Restraint stress elevates the plasma interleukin-6 levels in germ-free mice. J Neuroimmunol **115:**46–52.

40. **O'Mahony L, McCarthy J, Kelly P, Hurley G, Luo FY, Chen KS, O'Sullivan GC, Kiely B, Collins JK, Shanahan F, Quigley EMM.** 2005. *Lactobacillus* and *Bifidobacterium* in irritable bowel syndrome: symptom responses and relationship to cytokine profiles. Gastroenterology **128:**541–551.

41. **Ovreas L, Forney L, Daae FL, Torsvik V.** 1997. Distribution of bacterioplankton in meromictic Lake Saelenvannet, as determined by denaturing gradient gel electrophoresis of PCR-amplified gene fragments coding for 16S rRNA. Appl Environ Microbiol **63:**3367–3373.

42. **Pang W, Stradiotto D, Krych L, Karlskov-Mortensen P, Vogensen FK, Nielsen DS, Fredholm M, Hansen AK.** 2012. Selective inbreeding does not increase gut microbiota similarity in BALB/c mice. Lab Anim Epub ahead of print.

43. **Penders J, Stobberingh EE, Van den Brandt PA, Thijs C.** 2007. The role of the intestinal microbiota in the development of atopic disorders. Allergy **62:**1223–1236.

44. **Pepys MB, Hirschfield GM.** 2003. C-reactive protein: a critical update. J Clin Invest **111:**1805–1812.

45. **Pils MC, Bleich A, Fasnacht N, Bollati-Fogolin M, Schippers A, Rozell B.** 2011. Commensal gut flora reduces susceptibility to experimentally induced colitis via T-cell derived interleukin 10. Inflamm Bowel Dis **17:**2038–2046.

46. **Round JL, Mazmanian SK.** 2009. The gut microbiota shapes intestinal immune responses during health and disease. Nat Rev Immunol **9:**313–323.

47. **Rousseaux C, Thuru X, Gelot A, Barnich N, Neut C, Dubuquoy L, Dubuquoy C, Merour E, Geboes K, Chamaillard M, Ouwehand A, Leyer G, Carcano D, Colombel JF, Ardid D, Desreumaux P.** 2007. *Lactobacillus acidophilus* modulates intestinal pain and induces opioid and cannabinoid receptors. Nat Med **13:**35–37.

48. **Sheu MY, Fowler AJ, Kao J, Schmuth M, Schoonjans K, Auwerx J, Fluhr JW, Man MQ, Elias PM, Feingold KR.** 2002. Topical peroxisome proliferator-activated receptor α activators reduce inflammation in irritant and allergic contact dermatitis models. J Invest Dermatol **118:**94–101.

49. **Siqueira JF, Rocas IN, Rosado AS.** 2004. Investigation of bacterial communities associated with asymptomatic and symptomatic endodontic infections by denaturing gradient gel electrophoresis fingerprinting approach. Oral Microbiol Immunol **19:**363–370.

50. **Sudo N, Chida Y, Aiba Y, Sonoda J, Oyama N, Yu XN, Kubo C, Koga Y.** 2004. Postnatal microbial colonization programs the hypothalamic–pituitary–adrenal system for stress response in mice. J Physiol **558:**263–275.

51. **Tlaskalova-Hogenova H, Stepankova R, Hudcovic T, Tuckova L, Cukrowska B, Lodinova-Zadnikova R, Kozakova H, Rossmann P, Bartova J, Sokol D, Funda DP, Borovska D, Rehakova Z, Sinkora J, Hofman J, Drastich P, Kokesova A.** 2004. Commensal bacteria (normal microflora), mucosal immunity, and chronic inflammatory and autoimmune diseases. Immunol Lett **93:**97–108.

52. **Turnbaugh PJ, Ley RE, Mahowald MA, Magrini V, Mardis ER, Gordon JI.** 2006. An obesity-associated gut microbiome with increased capacity for energy harvest. Nature **444:**1027–1031.

53. **Watanabe S, Narisawa Y, Arase S, Okamatsu H, Ikenaga T, Tajiri Y, Kumemura M.** 2003. Differences in fecal microflora between patients with atopic dermatitis and healthy control subjects. J Allergy Clin Immunol **111:**587–591.

54. **Webb EF, Tzimas MN, Newsholme SJ, Griswold DE.** 1998. Intralesional cytokines in chronic oxazolone-induced contact sensitivity suggest roles for tumor necrosis factor α and interleukin 4. J Invest Dermatol **111:**86–92.

55. **Williams H, Stewart A, von Mutius E, Cookson W, Anderson HR.** 2008. Is eczema really on the increase worldwide? J Allergy Clin Immunol **121:**947–954.

56. **Wool GD, Reardon CA.** 2007. The influence of acute phase proteins on murine atherosclerosis. Curr Drug Targets **8:**1203–1214.

57. **Zhang T, Chen YD, Liu HB, Zhou ZH, Zhai YZ, Yang JJ.** 2010. Chronic unpredictable stress accelerates atherosclerosis through promoting inflammation in apolipoprotein E knockout mice. Thromb Res **126:**386–392.